Ceramics International xxx (xxxx) xxx

Contents lists available at ScienceDirect

Ceramics International

journal homepage: www.elsevier.com/locate/ceramint

Effect of extra added Mg^{2+} and Si^{4+} on the microstructure and luminescence properties of Ce:YAG ceramic phosphors for high power LED/LD lighting

Qian Zhang [a,b], Yun Shi [a,c,*], Denis Kosyanov [d], Yifei Xiong [a], Tong Wu [a], ZhenZhen Zhou [a], Qian Liu [a,c], Jinghong Fang [a], Jinqi Ni [a], Huan He [a], Jianding Yu [a,c], Mingjun Niu [b,**], Wentao Liu [b,***]

[a] State Key Laboratory of High Performance Ceramics and Superfine Microstructure, Shanghai Institute of Ceramics, Chinese Academy of Sciences, Shanghai, 200050, China
[b] School of Materials Science and Engineering, Zhengzhou University, Zhengzhou, 450001, China
[c] Center of Materials Science and Optoelectronics Engineering, University of Chinese Academy of Science, Beijing, 100049, China
[d] SEC "Advanced Ceramic Materials", Far Eastern Federal University, 10 Ajax Bay, Russky Island, Vladivostok, 690922, Russian Federation

ARTICLE INFO

Keywords:
Ce:YAG ceramic Phosphors
White LED
Sintering aids
Mg^{2+}
Si^{4+}

ABSTRACT

The study deals with the use of different amounts of MgO or tetraethyl orthosilicate ($C_8H_{20}O_4Si$, TEOS), from 0.04 wt %, 0.06 wt %, 0.08 wt %, 0.4 wt %, 0.6 wt % to 0.8 wt %, respectively, as additional sintering aids during the vacuum sintering of transparent Ce^{3+} doped $Y_3Al_5O_{12}$ (Ce:YAG) ceramics to investigate their effect on microstructure and luminescence properties. A comparative study was carried out by using X - ray diffraction, scanning electron microscopy/energy dispersive X - ray spectroscopy, optical and photo-luminesce spectra, as well as electroluminescent spectra. The dominant garnet phase was obtained even when adding 0.8 wt % of MgO or TEOS, while adding MgO led to finer average grain size (~ 5 - 10 μm) and more homogenous distribution compared to TEOS (~ 20 - 25 μm) in Ce:YAG ceramics. Adding a large amount of MgO was found to result in the segregation of MgO in Ce:YAG ceramics, while an excess of TEOS led to the segregation of Al_2O_3. A strong absorption peak at 308 nm was observed in Ce:YAG ceramics with MgO sintering aids, which was ascribed to the existence of Ce^{4+} induced by a charge compensation effect of Mg^{2+}. The optimum transmittance reached 80% @ 800 nm in Ce:YAG ceramics when adding 0.6 wt % TEOS, which also exhibited a maximum luminous efficacy of 106 lm/W. Si^{4+} was experimentally proved to have a better optimization effect on luminous efficacy compared to Mg^{2+}.

1. Introduction

Ce:YAG is a classical luminescence material, which has a long history of study [1]. It can be used as a highly efficient phosphor in white light-emitting diode (LED) or laser diode (LD) lighting [2], or as a scintillator in high-resolution X - ray imaging [3] or high energy physics [4], and even in solar cells [5], etc. Moreover, the YAG matrix possesses excellent thermal (13.4 W/mK) [6] and mechanical properties (Young's E 280 GPa) [6]. In recent years, due to the development of high-power LED/LD lighting [7,8], bulk phosphors, such as transparent ceramics [8–10], composite ceramics [11,12], glass ceramics [13,14], and single crystals [15] have attracted worldwide research interest due to their superior thermal conductivity as compared to organic epoxy resin or silicone. Among those, Ce:YAG transparent ceramics were actively studied from the fabrication method [9,16] to composition engineering [17,18]. They were considered to possess advantages over glass ceramics or single crystals for higher luminescent efficiency, lower fabrication temperature, mass production and the feasibility of composite

* Corresponding author. State Key Laboratory of High Performance Ceramics and Superfine Microstructure, Shanghai Institute of Ceramics, Chinese Academy of Sciences, Shanghai, 200050, China.
** Corresponding author.
*** Corresponding author.
E-mail addresses: shiyun@mail.sic.ac.cn (Y. Shi), niumj@zzu.edu.cn (M. Niu), wtliu@zzu.edu.cn (W. Liu).

https://doi.org/10.1016/j.ceramint.2022.11.331
Received 28 September 2022; Received in revised form 25 November 2022; Accepted 28 November 2022
Available online 30 November 2022

Table 1
The name list of Ce:YAG ceramics sintered with different amounts of sintering aids of MgO or TEOS, respectively, and their corresponding abbreviations.

Sintering aids amount (wt. %)	abbreviations name of 0.5 at. % Ce:YAG ceramics and the mole ratio of sintering aids ions with Ce^{3+}			
	MgO	Mg^{2+}/Ce^{3+}	TEOS	Si^{4+}/Ce^{3+}
0.04	CYM1	0.39	CYS1	0.08
0.06	CYM2	0.59	CYS2	0.11
0.08	CYM3	0.79	CYS3	0.15
0.4	CYM4	3.93	CYS4	0.76
0.6	CYM5	5.90	CYS5	1.14
0.8	CYM6	7.87	CYS6	1.52

structure design [19,20].

Sintering aids were commonly used to produce transparent ceramics. In the 1950s, Coble [21] demonstrated a pioneering fabrication of translucent Al_2O_3 ceramics by adding a small amount of MgO as a sintering aid. In the 1980s, de With and van Dijk [22] reported the first use of SiO_2 doping to achieve translucent YAG ceramics. Since then, MgO and TEOS were most commonly used as sintering aids during the fabrication of YAG transparent ceramics to promote densification, lower the numbers of scattering sources, such as pores, improve optical transmittance and homogeneity, etc. After investigated the addition features of MgO (0.01 - 0.15 wt %) in YAG transparent ceramics, the solubility limit of MgO was proposed to be 0.06 wt % and Mg^{2+} most likely substituted Al^{3+} sites, while exceeding the solubility limit led to the precipitation of spinel secondary phases [23]. The study on 0.03 wt % - 0.18 wt % MgO-assisted densification of YAG ceramics revealed that the optimum transmittance was obtained when adding 0.03 wt % MgO. With a further increase of MgO, significant grain growth occurred along with the generation of intragranular pores, as well as the Mg-rich secondary phase, which deteriorated the optical properties of YAG ceramics [24]. Meanwhile, the effect of TEOS on YAG transparent ceramics was also reported, especially in Nd:YAG laser ceramics [25,26]. TEOS decomposes to SiO_2, H_2O, and CO_2 at high temperatures, Si^{4+} was considered to be able to substitute onto tetrahedrally coordinated Al^{3+} sites during densification as long that solubility limit is not exceeded [26], the content of SiO_2 would increase both densification and grain growth rate at a lower temperature and second phases crystalline forms when Si^{4+} no longer soluble.

Furthermore, as an external additive outside the chemical stoichiometric, sintering aids were noticed to have effects on not only microstructure but also luminescence properties [27–29]. Mg^{2+} was generally found to be able to shorten the scintillation decay while decrease the luminescence efficiency, such as in Ce^{3+} or Pr^{3+} doped $Lu_3Al_5O_{12}$ (LuAG) [30–32], $(Gd,Lu)_3Al_5O_{12}$ (GLAG) [33], $Gd_3(Al,Ga)_5O_{12}$ (GGAG) scintillators [34–36]. A blueshift emission in Si^{4+} doped Ce:YAG was found which was attributed to a decrease in the splitting of 5*d* levels of the Ce^{3+} ion and the thermal stability was greatly improved [37]. Besides, 5 wt % SiO_2 - added Ce:YAG ceramic phosphors exhibited an increased quantum efficiency (more than 15%) and higher thermal stability (a 10% increase at 150 °C) compared to pristine Ce:YAG, it was attributed to a denser microstructure and an increase in thermal activation energy by Si substitution of Al in the host [38]. It was also found that moderate Si-codoping is efficient in reinforcing the radiation hardness and scintillation properties of Ce:YAG crystals [39].

The effect of MgO and TEOS as compound sintering aids was also studied in YAG, LuAG [32] and GdYAG [40] et al.. Compared to the single-used MgO or TEOS sintering aids, ceramics with compound sintering aids were found to exhibit better transparency and more homogeneous grains [41]. Meanwhile, high luminescence efficiency of 93.6 lm/W (blue light LED excitation) and 178.5 lm/W (blue light LD excitation) can be obtained in Ce:YAG ceramics with compound MgO (0.08 wt%) and TEOS (0.8 wt%) additives [42]. However, interaction between Mg^{2+} and Si^{4+} ions was also found to exist during the sintering of YAG ceramics [43]. Furthermore, due to the similar ion radius with Al^{3+}, Mg^{2+} and Si^{4+} can also solute into the YAG matrix and act as substitutions. $Ce:Y_3Mg_xAl_{5-2x}Si_xO_{12}$ (Ce:YAMSG) and $Ce^{3+}:Lu_3(Al,Mg)_2(Al,Si)_3O_{12}$ (Ce:LuAMSG) transparent ceramic phosphors have been developed successively [12,17,18,44,45]. It is found that the ion pair substitution of Mg^{2+} - Si^{4+} to Al^{3+} - Al^{3+} can reduce the sintering temperature, shrink the energy bandgap and enhance the crystal field (CF), and correspondingly low the 5d level of Ce^{3+} to introduce luminescence redshift. However, the absolute quantum efficiency of Ce^{3+} emission and the luminescence stability at high temperature decreases.

In summary, all the above works indicated the existed effect of MgO and SiO_2 for the optimization and application of YAG or other aluminate garnet transparent ceramics, we also noticed that the adding amount of MgO (0–0.2 wt %) was usually one order of magnitude lower than that of TEOS (0.5 - 1.0 wt %) in the previous studies. It might due to the solubility limit of Mg^{2+} in YAG is considered to be around 0.06 wt % [23]. Considering the proper amount of second phase particles can change the direction of light propagation in ceramics which may increase the absorption of excited light and the extraction of emitting light [40], we extended the adding amount of both MgO and TEOS to a wider range, and focused on the effects of MgO and TEOS as single sintering aids, respectively, in Ce:YAG ceramics by the vacuum sintering method, i.e. varying by one order of magnitude, the resultant microstructure, optical, and luminescence properties of Ce:YAG transparent ceramics were characterized to clarify the mechanism of sintering aids.

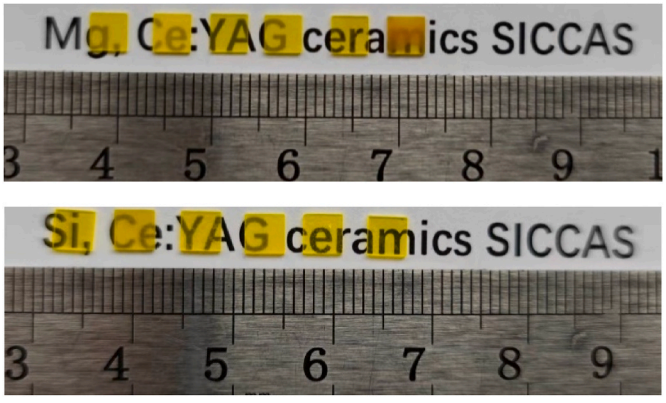

Fig. 1. Photograph of the Ce:YAG ceramics sintered with different amounts of sintering aids, CYM 1–6 (top row) or CYS 1–6 (bottom row); each dimension is 4 × 4 × 0.5 mm^3, double face polished, the additive amount is 0.04, 0.06, 0.08, 0.4, 0.6, and 0.8 wt % (from left to right), respectively.

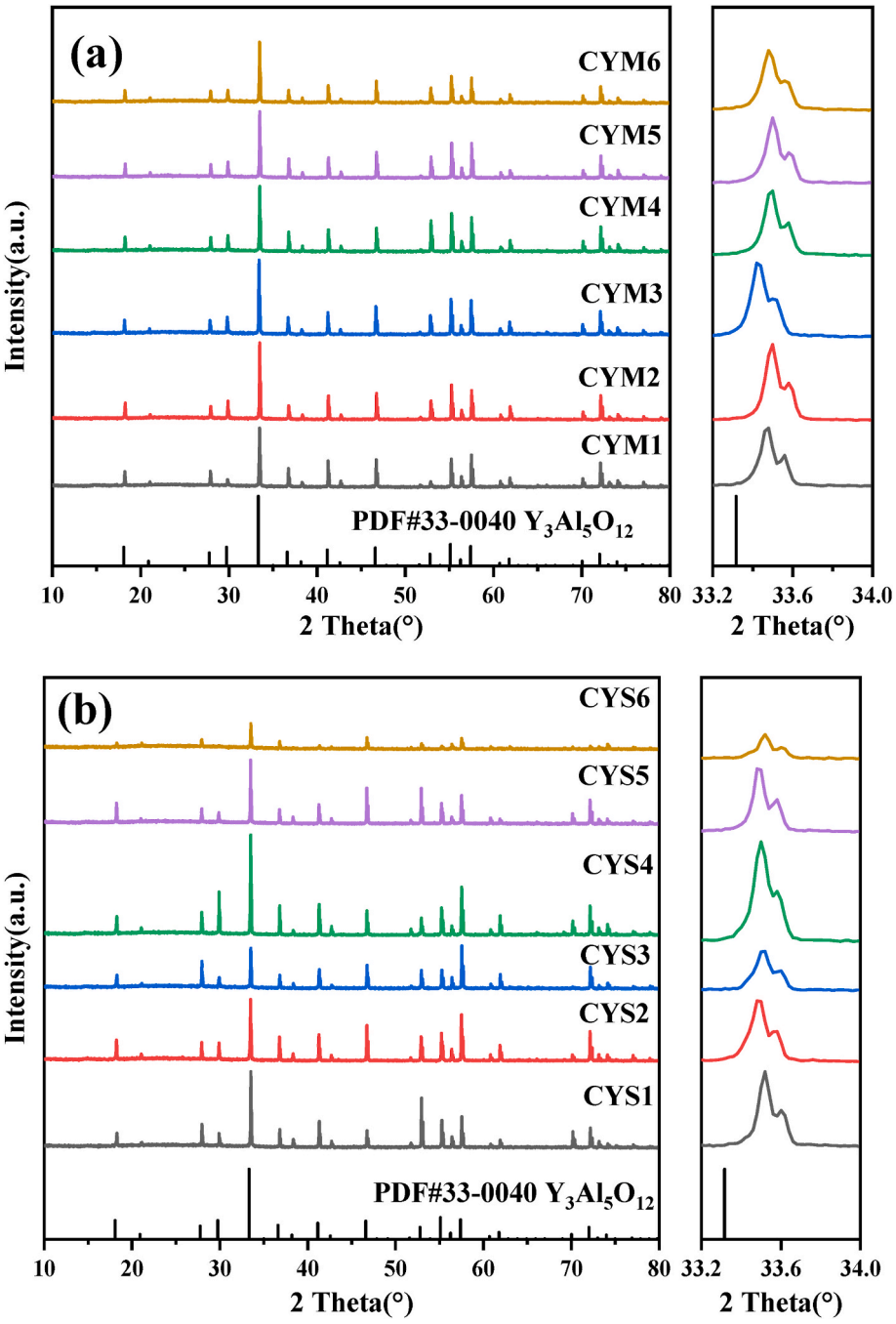

Fig. 2. XRD patterns of the Ce:YAG ceramics with different amounts of sintering aids (a) CYM 1–6; (b) CYS 1 - 6.

2. Experimental process

2.1. Ceramics fabrication

Ce:YAG ceramics were fabricated by the solid-state reaction method through vacuum sintering. High-purity commercial powders, α-Al_2O_3 (>99.99%), Y_2O_3 (>99.99%) and CeO_2 (>99.99%), were used as raw materials. They were weighted according to the chemical stoichiometry of $(Ce_{0.005}Y_{0.995})_3Al_5O_{12}$, i.e. 0.5 at. % Ce^{3+} doped YAG. High-purity MgO powders and TEOS solvent were used as external additives outside the chemical stoichiometry of Ce:YAG. As mentioned before, the TEOS would decompose SiO_2, H_2O, and CO_2 at high temperatures and the SiO_2 would act as sintering aids finally. The adding amount was 0.04 wt %, 0.06 wt %, 0.08 wt %, 0.4 wt %, 0.6 wt %, 0.8 wt %, respectively. The as-sintered Ce:YAG ceramics were named CYM and CYS and numbered according to the additive amounts of MgO or TEOS which are listed in Table 1, where their relative molar ratio with respect to Ce^{3+} were calculated and listed.

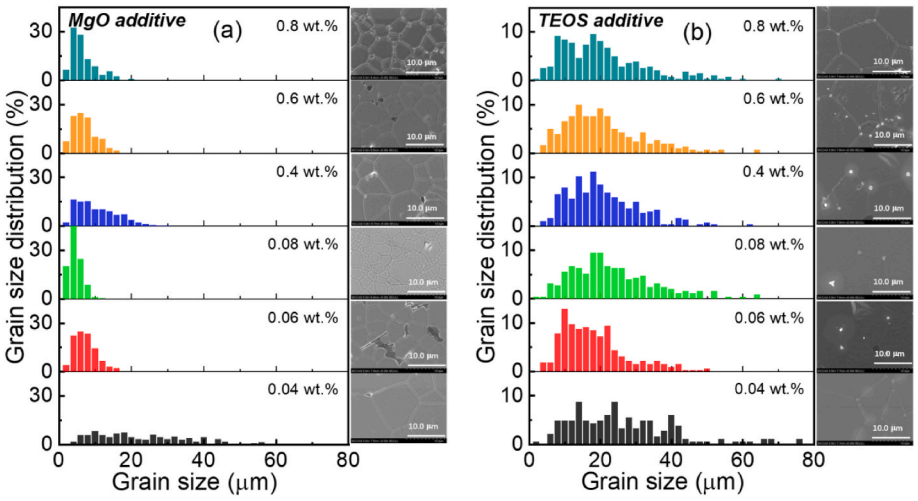

Fig. 3. The grain size morphology of the Ce:YAG ceramics with different amounts of sintering aids by SEM and their calculated grain size distribution. (a) CYM 1 - 6; (b) CYS 1 - 6.

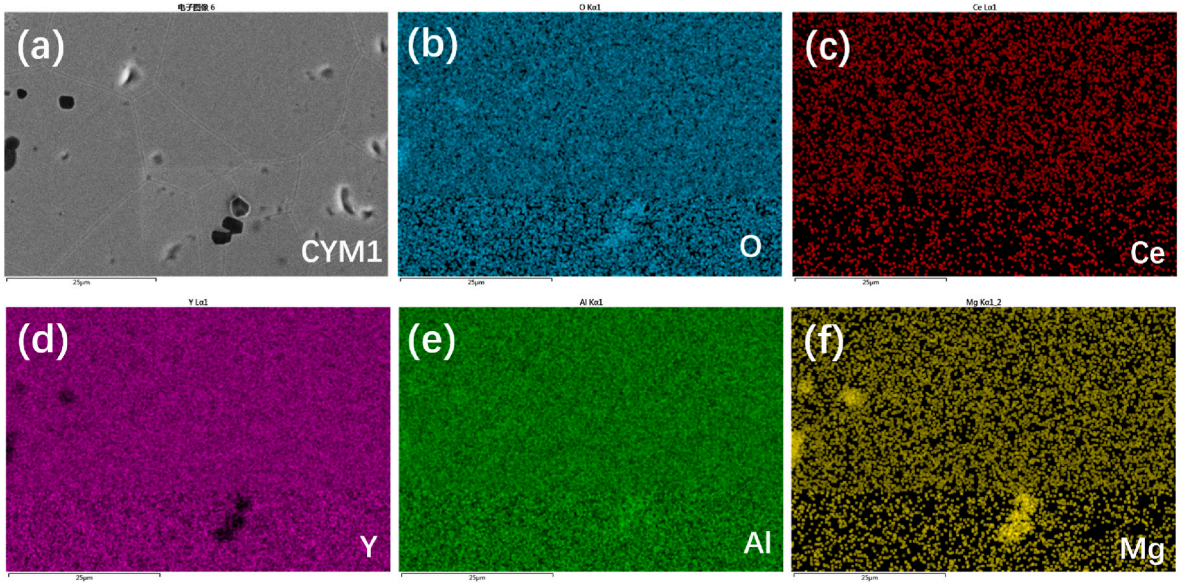

Fig. 4. The map scanning of elements distribution in the Ce:YAG ceramics with 0.04 wt% MgO sintering aids (CYM1, 0.04 wt %) characterized by SEM - EDS. (a) SEM morphology; (b) O elements; (c) Ce elements; (d) Y elements; (e) Al elements; (f) Mg elements.

The above-mentioned powders were mixed by a high-energy ball mill apparatus at 200 rpm for 12 h using alcohol as the ball milling medium. The slurry was dried in the air at 70 °C for 1 – 2 h and then sieved by a 200-mesh griddle. The obtained powders were calcined at 600 °C for 4 h in a muffle furnace to eliminate the possibly introduced organic impurities. Ceramic green bodies with dimensions of Φ 25 mm × 2 mm were formed by a 4 MPa uniaxial press and 200 MPa cold isostatic press, sequentially. The ceramic green bodies were sintered in a pressureless vacuum furnace at a temperature of 1750 °C for 20 h. The vacuum reached down to 10^{-4} Pa during the temperature holding process. The as-sintered ceramics were then cut and double-face polished to an optical grade to the dimension of 4 × 4 × 0.5 – 0.8 mm^3 for further measurements.

2.2. Characterization

The ceramic phase was determined by X - ray diffraction (XRD) measurement using an Ultima IV diffractometer (Cu Kα, 40 kV, 40 mA; Rigaku Corp., Japan) with a step size of 0.02° in a 2θ range of 10 - 80° and a scan rate of 2°/min. The images showing the grain size

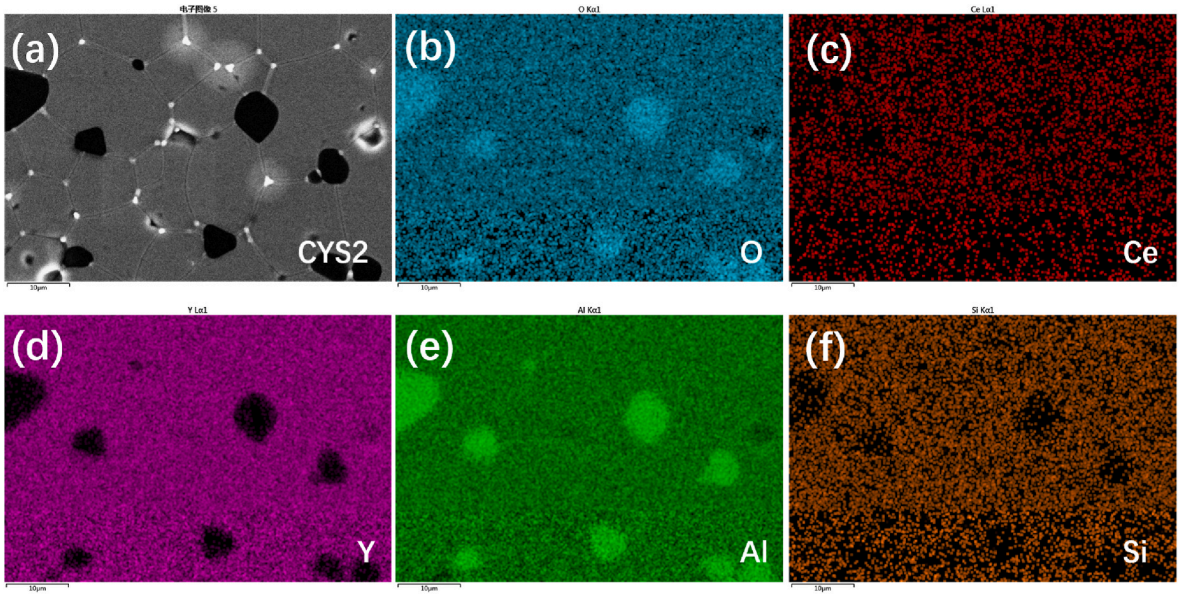

Fig. 5. Map scanning of elements distribution in the Ce:YAG ceramics with 0.06 wt % TEOS sintering aids (CYS2, 0.06 wt %) characterized by SEM - EDS. (a) SEM morphology; (b) O elements; (c) Ce elements; (d) Y elements; (e) Al elements; (f) Si elements.

morphology and map scanning of elements distribution in the Ce:YAG ceramics were characterized by a high-resolution scanning electron microscope (HR - SEM) S - 3400 N equipped with an energy dispersive X-ray spectroscope (EDS) (Hitachi Ltd., Japan). Before the SEM test, the Ce:YAG ceramics were double-face polished and thermally etched in the air at 1500 °C for 3 h. Grain size distribution of thermally etched ceramics was determined by using the linear intercept method. A correction factor of 1.56 was used to convert average intercept length to real grain sizes. Average grain size was determined from obtained distribution. At least 300 grains were analyzed for each measurement.

The absorption spectra were measured using a UV–Vis–NIR spectrophotometer Cary 5000 (Varian Medical System Inc., USA), and the apparatus baseline was subtracted automatically. Photoluminescence emission (PL) and excitation (PLE) spectra were recorded on a fluorescence spectrophotometer F - 4600 (Hitachi Ltd., Japan) with a scan rate of 1200 nm/min, with a xenon lamp as a light source. The electroluminescent (EL) properties, including EL spectra, Correlated Color Temperature (CCT), Commission Internationale de l'Éclairage (CIE) color coordinate, Color Rendering Index (CRI), and luminous efficacy, were measured using a spectroradiometer PM - 80V1 for LEDs with an integrating sphere (Everfine Co., China); the ceramics were excited by a commercial blue LED chip with 445 nm wavelength.

The LD luminous flux was recorded using an integrated optical and electrical meter (YF - 1000 high accuracy array spectroradiometer, PM-50 UV – VS - NIR spectroscopy analysis system; Everfine Co., China). The excitation source was a blue LD chip (450 nm, 1.4 W); the laser was focused on the ceramics in a φ 2 mm area range.

3. Results and discussion

Fig. 1 is the photograph of the as-sintered 0.5 at. % Ce:YAG ceramics. It can be seen that all of them reached visible transparency after double-face polishing. The color of CYM ceramics changed gradually from yellow to orange with increasing MgO addition while CYS ceramics retained yellow color. The dark color may be ascribed to the oxygen vacancies caused by the divalent cations (Mg^{2+}) [29,46] or the reduced fabrication environment of the ceramics [32]. Some works also found that the increased splitting of the Ce^{3+} 5*d* configuration may be caused by the substitution of Al^{3+} with Mg^{2+} [47], but CF caused strength variation may only change the hue. The detailed mechanism will be illustrated by the following characterizations.

Fig. 2 shows the XRD patterns of the as-sintered 0.5 at. % Ce:YAG transparent ceramics with different amounts of sintering aids (MgO or TEOS). The crystalline phases of all the ceramics were well indexed by the cubic YAG phase (PDF # 033–0040). The enlarged view of a prominent peak shows the diffraction angular shifting towards higher angles with respect to standard YAG phase. This angular shifting leads to decrease of the cell parameters. Mg^{2+}/Si^{4+} did not result in any significant changes in the host structure and no detectable second phase was observed even when the sintering aids were heavily added to 0.8 wt%. It is also consistent with the previous works [48]. It was demonstrated that the YAG lattice structure could accommodate Mg^{2+}/Si^{4+} over a wide concentration range. The weakened XRD intensity in Ce:YAG ceramics with 0.8 wt % TEOS sintering aids, as shown in Fig. 2 (b), may be due to the possible vitrification tendency in the situation of heavy SiO_2 introduction [49,50]. However, it does not mean that there are no any second phase at all since the detect limit of XRD technology is around 1%. From the following SEM and EDS test we can find traces of impurities, as well as the segregations of Al_2O_3 and MgO, which means an existence of local nonstoichiometric or second phase (probably some spinel is formed).

Fig. 3 (a) presents the morphology of the Ce:YAG ceramics grains with different amounts of MgO sintering aids which were characterized by SEM. Grain size distribution and average grain size of constituent phases were furtherly calculated by the linear intercept method using the SEM images of the thermally etched surface of Ce:YAG ceramics. Comparatively, Ce:YAG ceramics with the addition of 0.08 wt% MgO or 0.8 wt% MgO exhibited the most homogenous grain size distribution morphology and almost pore-free microstructure. Besides, a small

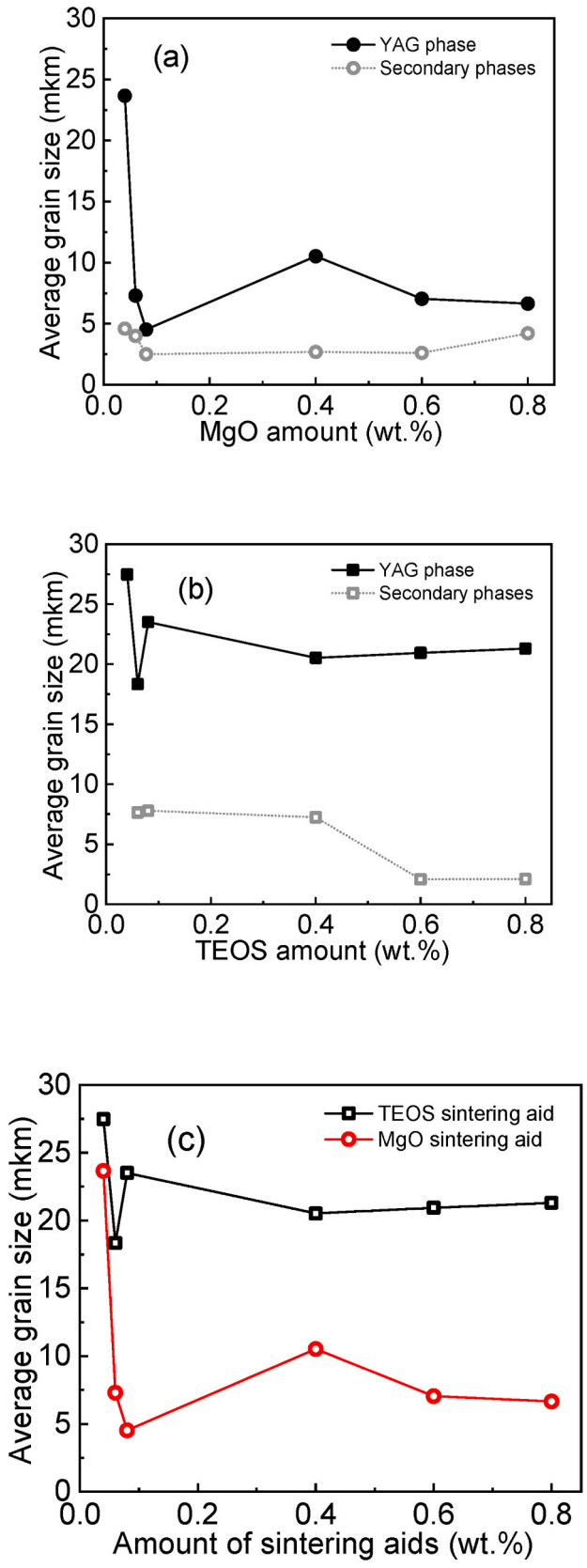

Fig. 6. Comparison of the calculated average grain size of the constituent phases for Ce:YAG ceramic samples with different sintering aids amounts of (a) MgO (CYM 1–6) and (b) TEOS (CYS 1–6); (c) generalized comparison for the matrix (YAG) phase.

amount of micropores could be observed in triple grain boundaries and inside grains, which would act as light scattering sources to degrade the in-line transmittance of transparent ceramics [51,52]. Correspondingly, the grain size morphology of Ce:YAG ceramics sintered with TEOS (Si^{4+}) additives is presented in Fig. 3(b). TEOS additives led to a significant increase in the grain size in Ce:YAG ceramics, much larger than in the MgO case. Unlike the case of MgO, TEOS introduced very small porosity but worse homogeneity. Si^{4+} thus is proved to promote both densification and grain growth rate effectively leading to coarsening-dominated grain growth in Ce:YAG ceramics.

As shown in Figs. 4 and 5, the map scanning of elements distribution in Ce:YAG ceramics with 0.04 wt% MgO or 0.06 wt% TEOS was recorded by SEM-EDS. By the comparison of the O element, Ce element, Y element, Al element, Mg element, and Si element, it can be seen clearly that there are Mg-rich regions in the ceramics even at the lowest MgO additive amount (0.04 wt %). Y, Al, and Ce elements were distributed homogenously in the detecting fields. Furthermore, Al-rich regions instead of Si-rich regions can be observed in the EDS map. Considering their ion radius relationship at 4 coordinator number sites, Si^{4+} (26 p.m.) < Al^{3+} (39 p.m.) < Mg^{2+} (57 p.m.) [53], one can suggest that Si^{4+} is more competitive during the substitution onto tetrahedrally coordinated Al^{3+} sites with respect to Mg^{2+} ions [26]. The shift of XRD peaks to higher angular, as shown in Fig. 2 (b), also support this proposal. Accordingly, Mg^{2+} (radius 89 p.m., 8 coordinator number) would tend to occupy the dodecahedron lattice site of Y^{3+} (radius 101.9 p.m., 8 coordinator number), and that's why there is also red shift of XRD peaks in Fig. 2 (a).

Fig. 6 shows their grain size distribution histograms for both CYM and CYS sample series. It can be seen that the grain size of CYMs is generally lower than that of CYSs, and the size distribution of the former is narrower, Mg^{2+} thus exhibited a more remarkable effect on inhibit grain growth than that of Si^{4+}. Therefore, an overall average grain size enhancement can be observed in ceramics with TEOS additives (~ 20 – 25 μm) compared to the MgO case (~ 5 – 10 μm) (see Fig. 6 c). It also can be seen that there are two stages of grain size evolution, i.e. an increase followed by a decrease, from 0.04 wt % MgO to 0.08 wt % MgO or from 0.4 wt % MgO to 0.8 wt % MgO, respectively. Mg^{2+} was commonly considered to have an inhibition effect on grain growth resulting from the solid solute drag effect during densification [23,24]. However, this work shows that such inhibition did not develop linearly with the Mg^{2+} concentration. It could be attributed to the competition of promoted densification [24,50]. The microstructure's evolution of the YAG phases differs more significantly. The average size of secondary phases is around: 2.5 – 4.5 μm and 2.5 – 7.5 μm for CYM and CYS sample series, respectively (see Fig. 6 a, b). In general, the quasi-spherical morphology corresponds to these impurities.

Fig. 7 shows the comparison of in-line transmittance and absorptance spectra in the visible light range of Ce:YAG ceramics (thickness 0.8 mm). The optimum transmittance of CYS ceramics reached up to ~ 80% @ 800 nm, which is higher than that in the CYM case (70% @ 800 nm). Generally, there are two absorption bands located at 350 nm and 450 nm, respectively, which made Ce:YAG proper phosphors for excitation of blue LED/LD chips. The transitions take place starting from a ground state $^2F_{5/2}$, resulting from the spin/orbital splitting of a $^4f_1$ configuration (which is further split by a cubic + tetragonal CF). The excitation (arrival states) stems from the $5d_1$ excited configuration. The ^2E_g ground level of such a configuration under a cubic CF is further split by the tetragonal part of the CF into a $^2A_{1g}$ and a $^2B_{1g}$ levels: the former is the arrival state for the 450 nm band and the latter for the 350 nm band [54].

Besides, this work also revealed that the absorptance character in the 250 – 450 nm range was dramatically different between CYM and CYS series ceramics, as shown in Fig. 7 (c), compared with CYS series ceramics, there was a strong absorption before 350 nm in CYM series ceramics. An obvious absorption peak located at around 308 nm was observed in CYM ceramics. The presence of the Ce^{4+} charge transfer

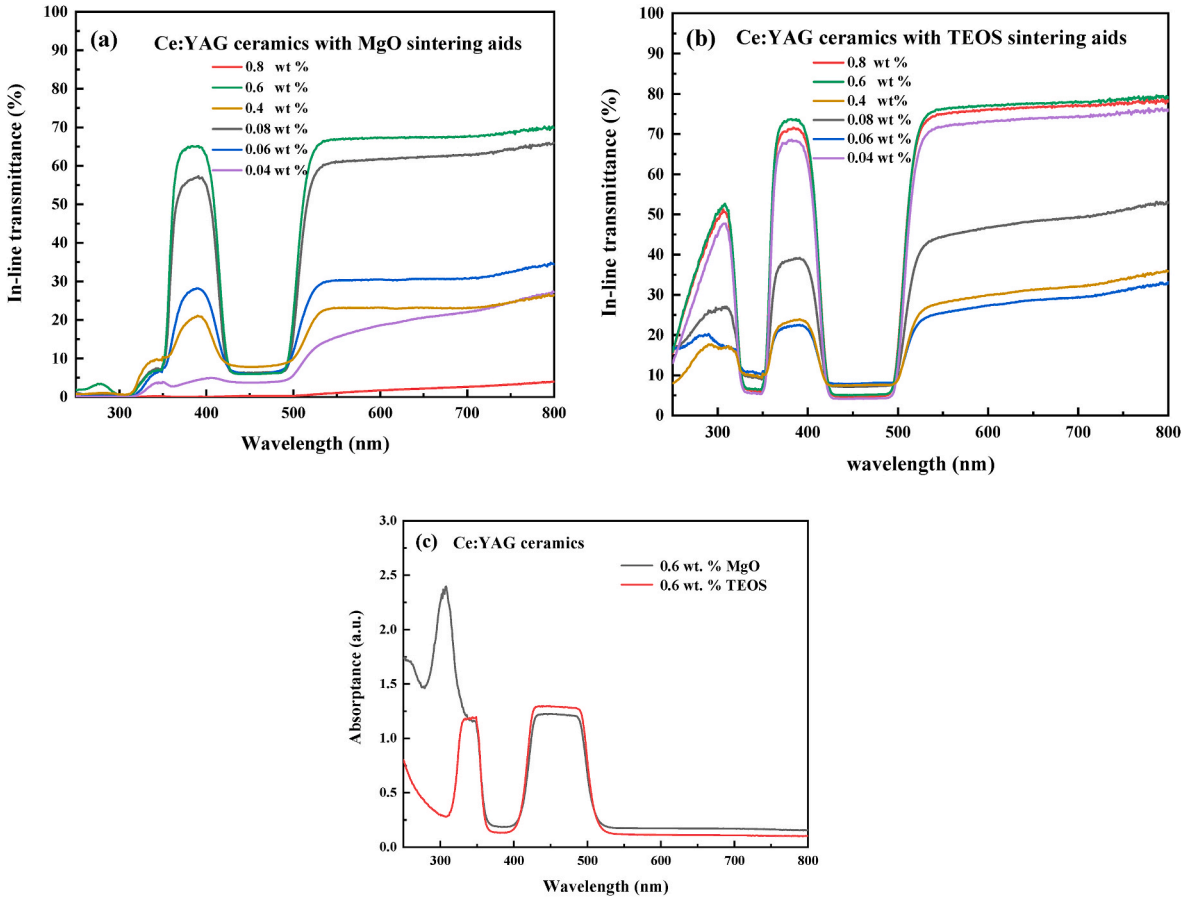

Fig. 7. Comparison of the in-line transmittance spectra of the Ce:YAG ceramics (thickness 0.8 mm), (a) CYM 1–6; (b) CYS 1–6, respectively. (c) Comparison of the absorptance spectra of CYM5 and CYS5.

(CT) absorption was reported to peak at about 240 nm in Ce, Mg:LuAG ceramics [32,55], and an additional absorption band around 300 nm was also ever reported in Ce:LuAG ceramics [56] without confirmation of the origin, however, considering the Ce^{4+} is a d_0 and f_0 cation, its bands are of the charge transfer type only viz and not influenced by the CF. One cannot attribute the 308 nm peak to Ce^{4+} in Ce:YAG ceramics and further mechanism need to be studied.

Fig. 8 shows the PLE ($\lambda_{em} = 530$ nm) and PL ($\lambda_{ex} = 450$ nm) spectra of the CYM and CYS series ceramics at room temperature. All of the ceramics have the excitation band at 350 nm and 450 nm which are characteristically attributed to the 4*f*-5*d* transition of Ce^{3+}. A broad emission peaking at around 530 nm also appeared in each CYM or CYS ceramics regardless of the sintering aids amount when excited by 450 nm wavelength light. It reveals that the adding of Mg^{2+} and Si^{4+} here does not introduce a change in the band gap of YAG or 5*d* levels of Ce^{3+}. Defect states were also reported to be missing in the YAG band gap [57]. The emission can be attributed to the transition of Ce^{3+} electrons from the 5*d* excited state to the $^2F_{5/2}$ and $^2F_{7/2}$ ground states [54]. It also demonstrated the solid solute of Ce^{3+} in the YAG matrix. CYM2 and CYS5, which have optimum room temperature PL intensities, were selected to investigate their thermal luminescence stability in the temperature range of RT – 225 °C, as shown in Fig. 9. It was found that the PL intensity decreased with an increase in temperature and 50% PL intensity could be kept at 225 °C. Besides, the PL intensity of CYM2 decreased almost linearly with an increase in temperature while CYS5 showed a two-step decrease with a sharper decrease at a temperature of below 100 °C. The mechanism of this process needs to be further studied.

The EL spectra of the Ce:YAG ceramics with different amounts of sintering aids of MgO or TEOS under blue chip excitation (445 nm) are shown in Fig. 10. CYM ceramics were found to have serious blue light leaks, while CYS ceramics absorbed the excited blue light sufficiently and the emission intensity was comparatively higher. Fig. 11 presents the comparison of the luminous efficacy of the Ce:YAG ceramics coupled with commercial blue LED chip excitation. It can be seen that the CYS ceramics have an overall enhancement of luminous efficacy with respect to CYM ceramics, 80 – 110 lm/W vs 20 – 70 lm/W. Reference Ce:YAG ceramic with compound sintering aids (0.08 wt % MgO +0.8 wt % TEOS) [42] was also shown here, and luminous efficacy was found to be located in the middle level compared with that of CYM and CYS series ceramics. A similar tendency is also shown in Fig. 12, which shows a comparison of the luminous flux of the Ce:YAG ceramics under blue LD chip excitation with an input power of 1.4 W. Table 2 summarizes the EL parameters of Ce:YAG ceramics under the excitation of a commercial blue LED chip with a wavelength of 445 nm. The emission of CYS ceramics exhibited a slight redshift (~ 5 – 10 nm) compared with CYM

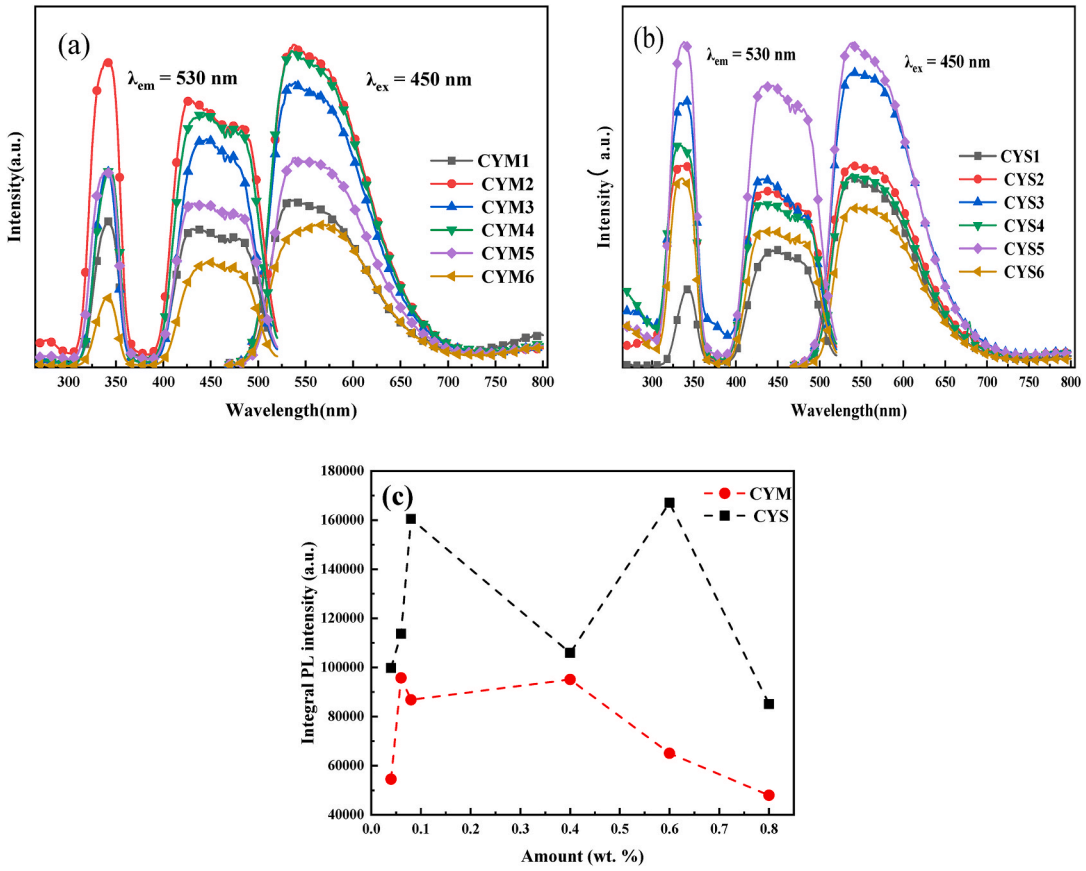

Fig. 8. PLE (λ_{em} = 530 nm) and PL (λ_{ex} = 450 nm) spectra of the Ce:YAG ceramics with different amounts of sintering aids of (a) MgO (CYM 1–6) and (b) TEOS (CYS 1–6); (c) The comparison of their integral PL intensity dependence with MgO or TEOS amounts.

ceramics. The maxim luminous efficacy (106.4 lm/W) occurred in CYS ceramics at the addition of 0.6 wt % TEOS, while for CYM ceramics, the maxim luminous efficacy occurred at the addition of 0.6 wt % MgO, although the value (68 lm/W) was comparatively lower than that of CYS. The high efficacy of ~106.4 lm/W and low CCT of 3742 K at the thickness of 0.5 mm is comparable to the single-surface textured Ce:YAG ceramics (93.0 lm/W, 4144K, 0.8 mm) [2] or transparent Ce:YAG ceramics (106 - 223 lm/W) [4].

In general, the red-light compensation and sufficient absorption of blue emitting light are still the import factors to improve both the luminous efficacy numbers and the quality of lighting. In this work, the CYS series ceramics exhibited a better lighting performance than that of CYMs which shows their potential in the future. The worse PL and EL performance of CYMs might be due to the insufficient absorption of blue light, the cation vacancies introduced by Mg^{2+} and corresponding charge compensation may possibly introduce point defects and formation of Ce^{4+} caused by Mg^{2+} compensation, for example, the emergence of $O_O^{\bullet}$ defects localized next to Mg^{2+} sites due to charge imbalance [34], as well as a decrease in Ce^{3+} owing to Ce^{4+} formation [55], whereas the former is the effective luminescence activator in Ce:YAG ceramics.

4. Conclusions

In summary, a series of Ce:YAG transparent ceramics were fabricated by the solid-state reaction method through vacuum sintering at 1750 °C for 20 h. The effect of extra Mg^{2+} and Si^{4+} addition on Ce:YAG ceramics was investigated. MgO or TEOS was added as additional sintering aids outside the chemical stoichiometric of Ce:YAG in a wide range, i.e. 0.04 wt %, 0.06 wt %, 0.08 wt %, 0.4 wt %, 0.6 wt %, and 0.8 wt %. The heavy addition of MgO was found to result in the segregation of MgO in Ce:YAG ceramics, while an excess of TEOS led to the segregation of Al_2O_3, which was ascribed to the competitive advantages of smaller Si^{4+} to bigger Mg^{2+} in substitution of Al^{3+} in tetrahedral site considering the matched degree of their ion radius. Besides, MgO proved to have a distinct inhibiting effect on grain growth and a worse optimization effect on luminous efficacy compared to TEOS. The maxim luminous efficacy occurred in 0.6 wt % TEOS (106 lm/W) or MgO (69 lm/W) added Ce:YAG ceramics, respectively, and their in-line transmittance also reached up to 80%. This comparison study on the effect of Mg^{2+} and Si^{4+} on luminescence performance sheds light on the rules to balance the optical transmittance and luminescence performance of Ce:YAG ceramics.

Declaration of competing interest

The authors declare that they have no known competing financial interests or personal relationships that could have appeared to influence the work reported in this paper.

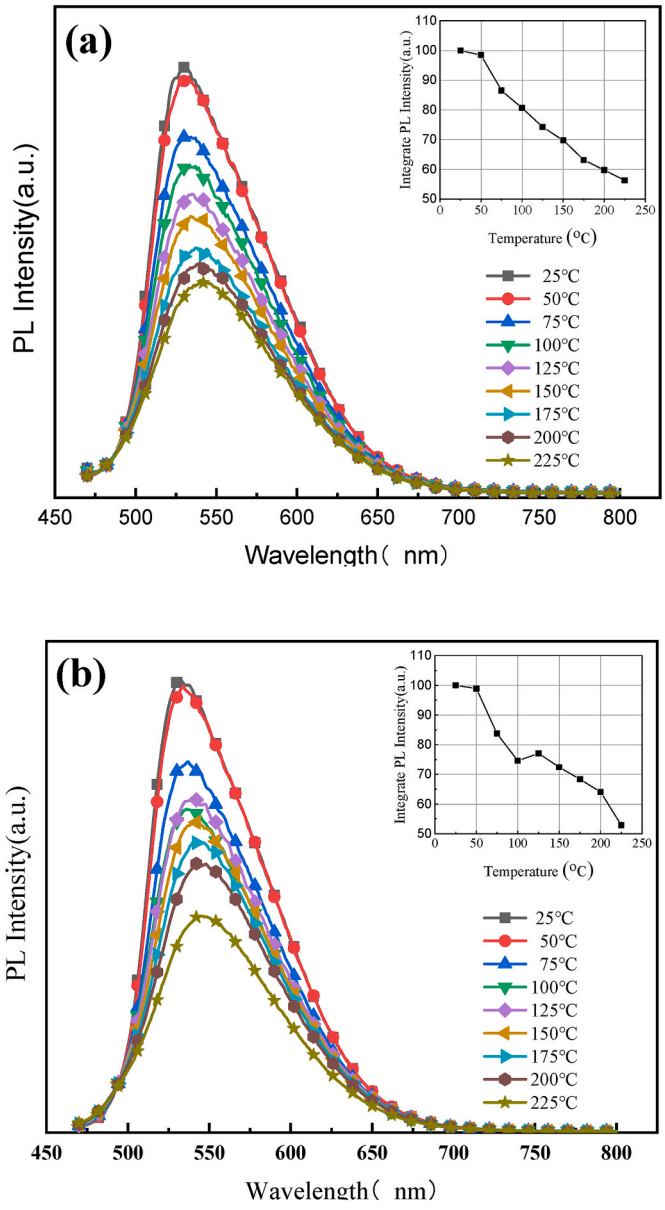

Fig. 9. The PL (λ_{ex} = 450 nm) spectra of CYM2 (a) and CYS5 (b) ceramics from 25 to 225 °C, the inset is the integral PL intensity dependence with temperatures.

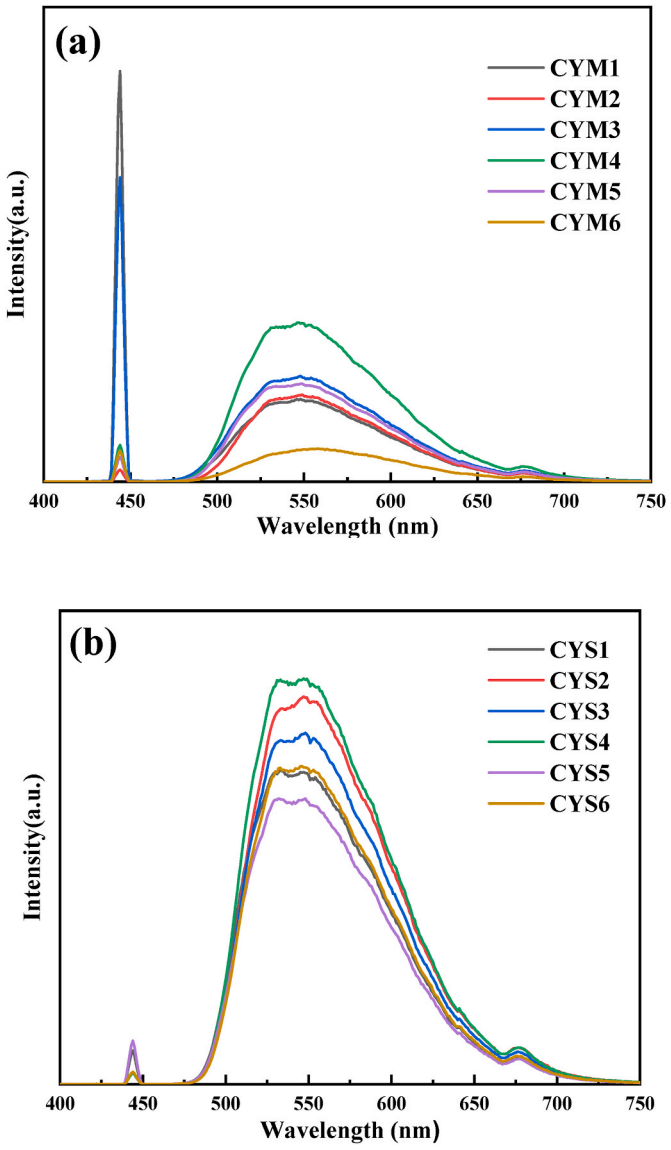

Fig. 10. EL spectra of the Ce:YAG ceramics with different amounts of sintering aids of (a) CYM 1–6; (b) CYS1-6 under blue LD chip excitation with an input power of 1.4 W, λ_{ex} = 450 nm. (For interpretation of the references to color in this figure legend, the reader is referred to the Web version of this article.)

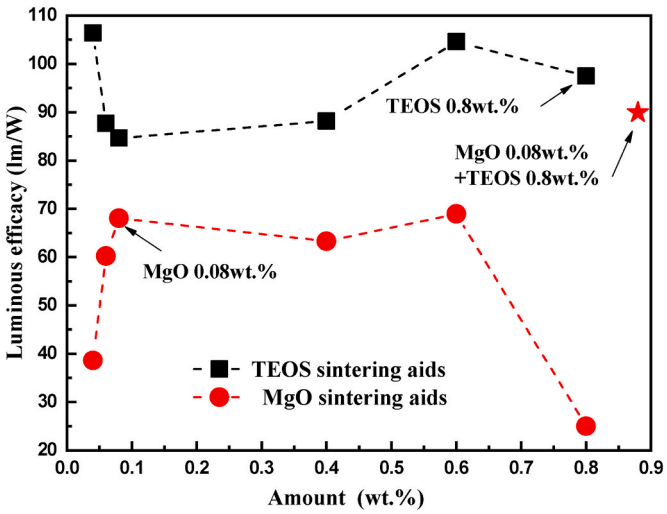

Fig. 11. Comparison of the luminous efficacy of the Ce:YAG ceramics under blue LED chip excitation, λ_{ex} = 445 nm. (For interpretation of the references to color in this figure legend, the reader is referred to the Web version of this article.)

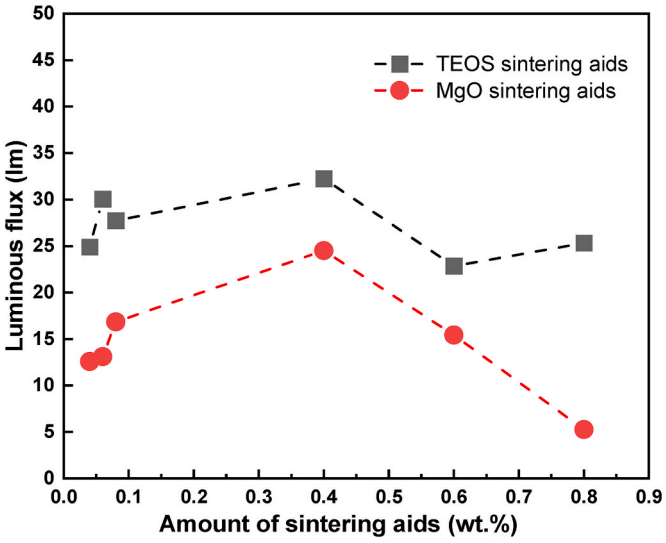

Fig. 12. Comparison of the luminous flux of the Ce:YAG ceramics under blue LD chip excitation with an input power of 1.4 W, λ_{ex} = 450 nm. (For interpretation of the references to color in this figure legend, the reader is referred to the Web version of this article.)

Table 2
The EL parameters of Ce:YAG ceramics under the excitation of a commercial blue LED chip with a wavelength of 445 nm.

Sintering aids amount (wt. %)		Luminous efficacy (lm/W)	color coordinate		CCT (K)	Emission peak (nm)	FWHM (nm)
			x	y			
Blue LED chip		13.46	0.1563	0.0209	100000	445	17.6
MgO	0.04	38.6	0.4066	0.515	4181	540	104.4
	0.06	60.24	0.4273	0.5378	3954	550	105
	0.08	68.05	0.4182	0.5213	4021	540	105.2
	0.4	63.28	0.429	0.5201	3853	545	103.8
	0.6	68.94	0.4241	0.5384	4003	540	103.4
	0.8	25.02	0.3834	0.4679	4417	535	111.1
TEOS	0.04	106.4	0.4402	0.5317	3742	545	100.4
	0.06	87.64	0.4365	0.5357	3813	560	109.6
	0.08	84.64	0.4298	0.5197	3839	550	108.2
	0.4	88.15	0.4398	0.5297	3740	545	109
	0.6	104.6	0.4402	0.5329	3749	545	100.8
	0.8	97.52	0.3949	0.4505	4109	545	100.8

Acknowledgement

The authors are thankful for the financial support from the National Natural Science Foundation of China (No. 62175249, 61475175); the Strategic Priority Research Program of the Chinese Academy of Sciences (XDA22010301); the Research Program of Shanghai Sciences and Technology Commission Foundation (22511100300, 19DZ1100703 and 18511110400). D. Yu. K. gratefully acknowledges the support from the Russian Science Foundation (Project No. 20-73-10242).

References

[1] Z.G. Xia, A. Meijerink, Ce^{3+}-Doped garnet phosphors: composition modification, luminescence properties and applications, Chem. Soc. Rev. 46 (2017) 275–299.
[2] L. Zhang, B. Sun, L. Gu, W. Bu, X. Fu, R. Sun, T. Zhou, F.A. Selim, C. Wong, H. Chen, Enhanced light extraction of single-surface textured YAG:Ce transparent ceramics for high power white LEDs, Appl. Surf. Sci. 455 (2018) 425–432.
[3] T. Ji, T. Wang, H. Li, Q. Peng, H. Tang, S. Hu, A. Yakovlev, Y. Zhong, X. Xu, Ce^{3+}-Doped yttrium aluminum garnet transparent ceramics for high-resolution X-ray imaging, Adv. Opt. Mater. 10 (2022), 2102056.
[4] O. Sidletskiy, K. Lebbou, D. Kofanov, Micro-pulling-down growth of long YAG- and LuAG-based garnet fibres: advances and bottlenecks, CrystEngComm 23 (2021) 2633–2643.
[5] A. Sidahmed, A. Kitai, Tandem Ce:YAG fluorescent solar concentrator, Sol. Energy Mater. Sol. Cells 145 (2016) 217–225.
[6] M.J. Weber, in: M.J. Weber (Ed.), Handbook of Optical Materials, CRC Press, 2003.
[7] J. Cho, J.H. Park, J.K. Kim, E.F. Schubert, White light-emitting diodes: history, progress, and future, Laser Photon. Rev. 11 (2017) 16001471–160014717.
[8] Q. Yao, P. Hu, P. Sun, M. Liu, R. Dong, K. Chao, Y. Liu, J. Jiang, H. Jiang, YAG:Ce^{3+} transparent ceramic phosphors brighten the next-generation laser-driven lighting, Adv. Mater. 32 (2020), e1907888.
[9] Y. Shi, P. Yubai, F. Xiqi, L. jiang, G. Jingkun, Fabrication and luminescence study of Ce^{3+} doped YAG transparent ceramics, J. Inorg. Mater. 25 (2010) 125–128.
[10] Y.F. Liu, S. Liu, P. Sun, Y.B. Du, S. Lin, R.J. Xie, R. Dong, J. Jiang, H.C. Jiang, Transparent ceramics enabling high luminous flux and efficacy for the next-generation high-power LED light, ACS Appl. Mater. Interfaces 11 (2019) 21697–21701.
[11] X. Liu, X. Qian, P. Zheng, X. Chen, Y. Feng, Y. Shi, J. Zou, R. Xie, J. Li, Composition and structure design of three-layered composite phosphors for high color rendering chip-on-board light-emitting diode devices, J. Adv. Ceram. 10 (2021) 729–740.
[12] S. Feng, Y. Guo, M. Allix, S. Li, R.-J. Xie, J. Fu, C. Genevois, E. Véron, H. Wang, Y. Yang, H. Qin, J. Li, Biphasic $Lu_3MgAl_3SiO_{12}$-based transparent ceramics for uniform laser-diode-driven white lighting, Cell Rep. Phys. Sci. 3 (2022), 101044.
[13] H. Lin, T. Hu, Y. Cheng, M.X. Chen, Y.S. Wang, Glass ceramic phosphors: towards long-lifetime high-power white light-emitting-diode applications-A review, Laser Photon. Rev. 12 (2018), 1700344.
[14] R. Zhang, H. Lin, Y. Yu, D. Chen, J. Xu, Y. Wang, A new-generation color converter for high-power white LED: transparent Ce3+:YAG phosphor-in-glass, Laser Photon. Rev. 8 (2014) 158–164.
[15] J. Xu, A. Thorseth, C. Xu, A. Krasnoshchoka, M. Rosendal, C. Dam-Hansen, B.L. Du, Y.X. Gong, O.B. Jensen, Investigation of laser-induced luminescence saturation in a single-crystal YAG:Ce phosphor: towards unique architecture, high saturation threshold, and high-brightness laser-driven white lighting, J. Lumin. 212 (2019) 279–285.
[16] X.G. Ma, X.Y. Li, J.Q. Li, C. Genevois, B.Q. Ma, A. Etienne, C.L. Wan, E. Veron, Z. J. Peng, M. Allix, Pressureless glass crystallization of transparent yttrium aluminum garnet-based nanoceramics, Nat. Commun. 9 (2018) 1175.

[17] Q.P. Du, S.W. Feng, H.M. Qin, H. Hua, H. Ding, L. Jia, Z.J. Zhang, J. Jiang, H. C. Jiang, Massive red-shifting of Ce^{3+} emission by Mg^{2+} and Si^{4+} doping of YAG:Ce transparent ceramic phosphors, J. Mater. Chem. C 6 (2018) 12200–12205.
[18] Y. Tian, Y. Tang, X. Yi, J. Chen, S. Sun, D. Zhao, H. Lin, S. Zhou, Optimization of Ce^{3+} concentration and $Y_4MgSi_3O_{13}$ phase in Mg^{2+}-Si^{4+} Co-doped Ce:YAG ceramic phosphors, J. Am. Ceram. Soc. 103 (2020) 6453–6460.
[19] G.L. Messing, A.J. Stevenson, Toward pore-free ceramics, Science 322 (2008) 383–384.
[20] A. Ikesue, Y.L. Aung, Ceramic laser materials, Nat. Photonics 2 (2008) 721–727.
[21] R.L. C, Preparation of transparent ceramic Al_2O_3, Am. Ceram. Soc. Bull. 38 (1959) 507.
[22] G.d. With, H.J.A. van Dijk, Translucent $Y_3Al_5O_{12}$ ceramics, Mater. Res. Bull. 19 (1984) 1669–1674.
[23] I. Vorona, A. Balabanov, M. Dobrotvorska, R. Yavetskiy, O. Kryzhanovska, L. Kravchenko, S. Parkhomenko, P. Mateychenko, V. Baumer, I. Matolinova, Effect of MgO doping on the structure and optical properties of YAG transparent ceramics, J. Eur. Ceram. Soc. 40 (2020) 861–866.
[24] T. Zhou, L. Zhang, S. Wei, L. Wang, H. Yang, Z. Fu, H. Chen, F.A. Selim, Q. Zhang, MgO assisted densification of highly transparent YAG ceramics and their microstructural evolution, J. Eur. Ceram. Soc. 38 (2018) 687–693.
[25] Y. Li, S. Zhou, H. Lin, X. Hou, W. Li, H. Teng, T. Jia, Fabrication of Nd:YAG transparent ceramics with TEOS, MgO and compound additives as sintering aids, J. Alloys Compd. 502 (2010) 225–230.
[26] A.J. Stevenson, X. Li, M.A. Martinez, J.M. Anderson, D.L. Suchy, E.R. Kupp, E. C. Dickey, K.T. Mueller, G.L. Messing, Effect of SiO_2 on densification and microstructure development in Nd:YAG transparent ceramics, J. Am. Ceram. Soc. 94 (2011) 1380–1387.
[27] Y. Shen, Y. Shi, X. Feng, Y. Pan, J. Li, Y. Zeng, M. Nikl, A. Krasnikov, A. Vedda, F. Moretti, The harmful effects of sintering aids in Pr: Lu AG optical ceramic scintillator, J. Am. Ceram. Soc. 95 (2012) 2130–2132.
[28] T.Y. Zhou, L. Zhang, H. Yang, X.B. Qiao, P. Liu, D.Y. Tang, J. Zhang, Effects of sintering aids on the transparency and conversion efficiency of Cr^{4+} ions in Cr: YAG transparent ceramics, J. Am. Ceram. Soc. 98 (2015) 2459–2464.
[29] A. Ikesue, Y.L. Aung, J. Klimke, Synthesis of Yb:YAG ceramics without sintering additives and their performance, J. Am. Ceram. Soc. 100 (2017) 26–30.
[30] X.P. Chen, Z.W. Hu, Y.G. Feng, X. Liu, H.H. Chen, Y. Shi, H.M. Kou, R. Kucerkova, A. Beitlerova, E. Mihokova, M. Nikl, J. Li, Electronic band modification for faster and brighter $Ce,Mg:Lu_{3-x}Y_xAl_5O_{12}$ ceramic scintillators, J. Lumin. (2019) 214.
[31] Z.W. Hu, M.Q. Cao, H.H. Chen, Y. Shi, H.M. Kou, T.F. Xie, L.X. Wu, Y.B. Pan, X. Q. Feng, A. Vedda, A. Beitlerova, M. Nikl, J. Li, The role of air annealing on the optical and scintillation properties of Mg co-doped Pr:LuAG transparent ceramics, Opt. Mater. 72 (2017) 201–207.
[32] Y. Shi, Y. Zhao, M. Cao, H. Chen, Z. Hu, X. Chen, Z. Zhang, Q. Liu, Dense Ce^{3+} doped $Lu_3A1_5O_{12}$ ceramic scintillators with low sintering adds: doping content effect, luminescence characterization and proton irradiation hardness, J. Lumin. 225 (2020), 117336.
[33] Q. Meng, X. Wang, Q. Zhu, J.-G. Li, The effects of Mg^{2+}/Si^{4+} co-substitution for Al^{3+} on sintering and photoluminescence of $(Gd,Lu)_3Al_5O_{12}$:Ce garnet ceramics, J. Eur. Ceram. Soc. 40 (2020) 3262–3269.
[34] K. Bartosiewicz, A. Markovskyi, T. Horiai, D. Szymański, S. Kurosawa, A. Yamaji, A. Yoshikawa, Y. Zorenko, A study of Mg^{2+} ions effect on atoms segregation, defects formation, luminescence and scintillation properties in Ce^{3+} doped $Gd_3Al_2Ga_3O_{12}$ single crystals, J. Alloys Compd. 905 (2022), 164154.
[35] Q. Qi, M. Meng, D.-z. Ding, S.-w. Zhao, J.-j. Shi, G.-h. Ren, Effects of trace MgO addition on optical and scintillation properties of GAGG:Ce crystal, Chin. J. Lumin. 42 (2021) 28–36.
[36] H. Ding, Z.H. Liu, Y.F. Liu, P. Hu, P. Sun, Z.H. Luo, K.F. Chao, H.C. Jiang, J. Jiang, $Gd_3Al_3Ga_2O_{12}$:Ce, Mg^{2+} transparent ceramic phosphors for high-power white LEDs/LDs, Ceram. Int. 47 (2021) 7918–7924.
[37] S.-Y. Xu, X.-S. Zhang, Y.-L. Zhou, Q. Xi, L. Li, Influence of Si^{4+} substitution on the temperature-dependent characteristics of $Y_3Al_5O_{12}$:Ce, Chin. Phys. B B 20 (2011), 037804.
[38] Y.T. Nien, J.K. You, Improved thermal quenching of $Y_3Al_5O_{12}$:Ce phosphor ceramics with silica addition, J. Alloys Compd. 678 (2016) 1–4.
[39] S. Baccaro, A. Cecilia, E. Mihokova, M. Nikl, K. Nejezchleb, K. Blazek, Influence of Si-codoping on YAG:Ce scintillation characteristics, IEEE Trans. Nucl. Sci. 52 (2004) 1105–1108.
[40] X. Liu, X. Qian, P. Zheng, Z. Hu, X. Chen, H. Pan, J. Zou, R. Xie, J. Li, Preparation and optical properties of $MgAl_2O_4$-Ce:GdYAG composite ceramic phosphors for white LEDs, J. Eur. Ceram. Soc. 39 (2019) 4965–4971.
[41] H. Yang, X. Qin, J. Zhang, J. Ma, D. Tang, S. Wang, Q. Zhang, The effect of MgO and SiO_2 codoping on the properties of Nd:YAG transparent ceramic, Opt. Mater. 34 (2012) 940–943.
[42] Z. Zheng, X. Zhang, X. Xu, Q. Liu, Y. Shi, R. Li, H. Wang, F. Wang, G. Liu, Thickness and surface roughness effect on lighting performance of Ce^{3+}: YAG transparent ceramics based high power LED and LD lighting prototype devices, Chin. J. Lumin. 41 (2020) 1411–1420.
[43] I.O. Vorona, R.P. Yavetskiy, S.V. Parkhomenko, A.G. Doroshenko, O. S. Kryzhanovska, N.A. Safronova, A.D. Timoshenko, A.E. Balabanov, A. V. Tolmachev, V.N. Baumer, Effect of complex Si^{4+} + Mg^{2+} additive on sintering and properties of undoped YAG ceramics, J. Eur. Ceram. Soc. 42 (2022) 6104–6109.
[44] H. Ji, L. Wang, M.S. Molokeev, N. Hirosaki, R. Xie, Z. Huang, Z. Xia, O.M.t. Kate, L. Liu, V.V. Atuchin, Structure evolution and photoluminescence of $Lu_3(Al,Mg)_2(Al,Si)_3O_{12}:Ce^{3+}$ phosphors: new yellow-color converters for blue LED-driven solid state lighting, J. Mater. Chem. C 4 (2016) 6855–6863.
[45] Q. Meng, J.-G. Li, Q. Zhu, X. Li, X. Sun, The effects of Mg^{2+}/Si^{4+} substitution on crystal structure, local coordination and photoluminescence of $(Gd,Lu)_3Al_5O_{12}$:Ce garnet phosphor, J. Alloys Compd. 797 (2019) 477–485.
[46] O. Sidletskiy, K. Lebbou, D. Kofanov, V. Kononets, I. Gerasymov, R. Bouaita, V. Jary, R. Kucerkova, M. Nikl, A. Polesel, K. Pauwels, E. Auffray, Progress in fabrication of long transparent YAG:Ce and YAG:Ce,Mg single crystalline fibers for HEP applications, CrystEngComm 21 (2019) 1728–1733.
[47] Q. Du, S. Feng, H. Qin, H. Hua, H. Ding, L. Jia, Z. Zhang, J. Jiang, H. Jiang, Massive red-shifting of Ce^{3+} emission by Mg^{2+} and Si^{4+} doping of YAG:Ce transparent ceramic phosphors, J. Mater. Chem. C 6 (2018) 12200–12205.
[48] B. Sun, L. Zhang, T. Zhou, C. Shao, L. Zhang, Y. Ma, Q. Yao, Z. Jiang, F.A. Selim, H. Chen, Protected-annealing regulated defects to improve optical properties and luminescence performance of Ce:YAG transparent ceramics for white LEDs, J. Mater. Chem. C 7 (2019) 4057–4065.
[49] M.G. Gong, W.D. Xiang, J. Huang, C.F. Yin, X.J. Liang, Facile synthesis and optical properties of Ce:YAG polycrystalline ceramics with different SiO_2 content, RSC Adv 5 (2015) 75781–75786.
[50] S.-H. Lee, E.R. Kupp, A.J. Stevenson, J.M. Anderson, G.L. Messing, X. Li, E. C. Dickey, J.Q. Dumm, V.K. Simonaitis-Castillo, G.J. Quarles, Hot isostatic pressing of transparent Nd:YAG ceramics, J. Am. Ceram. Soc. 92 (2009) 1456–1463.
[51] W. Ming, Z. Jiang, G. Luo, Y. Xu, W. He, Z. Xie, D. Shen, L. Li, Progress in transparent nano-ceramics and their potential applications, Nanomaterials 12 (2022) 1491.
[52] A. Ikesue, Y.L. Aung, T. Taira, T. Kamimura, K. Yoshida, G.L. Messing, Progress in ceramic lasers, Annu. Rev. Mater. Res. 36 (2006) 397–429.
[53] J.G. Speight, LANGE'S Handbook of Chemistry, sixteenth ed., CD&W Inc., Laramie, Wyoming, 2008.
[54] G. Blasse, A. Bril, Investigation of some Ce^{3+}-activated phosphors, J. Chem. Phys. 47 (1967) 5139–5145.
[55] S.P. Liu, J.A. Mares, X.Q. Feng, A. Vedda, M. Fasoli, Y. Shi, H.M. Kou, A. Beitlerova, L.X. Wu, C. D'Ambrosio, Y.B. Pan, M. Nikl, Towards bright and fast $Lu_3Al_5O_{12}$:Ce, Mg optical ceramics scintillators, Adv. Opt. Mater. 4 (2016) 731–739.
[56] M. Nikl, J.A. Mares, N. Solovieva, H.L. Li, X.J. Liu, L.P. Huang, I. Fontana, M. Fasoli, A. Vedda, C. D'Ambrosio, Scintillation characteristics of $Lu_3Al_5O_{12}$:Ce optical ceramics, J. Appl. Phys. 101 (2007).
[57] S. Jiang, T. Lu, J. Chen, Ab initio study the effects of Si and Mg dopants on point defects and Y diffusion in YAG, Comput. Mater. Sci. 69 (2013) 261–266.